JOURNAL OF MOLECULAR SPECTROSCOPY 152, 13–28 (1992)

Submillimeter-Wave Spectrum of H_2Se: The Evidence of Fourfold Clustering of Rotational Levels

I. N. KOZIN, S. P. BELOV, O. L. POLYANSKY, AND M. YU. TRETYAKOV

Institute of Applied Physics, USSR Academy of Science, Nizhny Novgorod, USSR

The spectra of $H_2{}^{80}Se$ and $H_2{}^{78}Se$ were investigated in the region 300–650 GHz including transitions with high rotational excitation up to $J = 20$, $K_{-1} = 20$. The effect of fourfold clustering of rotational energy levels was observed and interpreted as a critical phenomenon. Very strong distortion of line strengths was also found for rotational transitions in the region of critical phenomena. The measured frequencies were fitted, together with available MW data and IR ground state combination differences, in the modified Watson Hamiltonian and the sets of rotational and centrifugal distortion constants were obtained. © 1992 Academic Press, Inc.

INTRODUCTION

Centrifugal distortion plays an important role in molecular rovibrational spectra. As a rule it is treated in the theory by means of effective rotational Hamiltonians (*1*). In this way one can easily find the centrifugal correction to the rigid rotor model.

Allowing for the centrifugal perturbation can result not only in quantitative but also in qualitative changes in the spectrum. The cluster structure of rotational spectra of spherical top molecules (*2*) is a well-known example. The series of studies by Harter and Patterson (*3, 4* and references therein) was devoted to the cluster structure of rotational spectra of molecules with different types of symmetry. Recent progress has been made by Pavlichenkov and Zhilinskii (*5*). They showed that centrifugal perturbation can also rearrange the cluster structure with the increase of the total angular momentum J and that this effect corresponds to bifurcation in a classical Hamiltonian. Investigations and analysis of rovibrational spectra (*6–8*) have led to the conclusion that the phenomena called critical by the authors actually take place for spherical top molecules. Model calculations for the water molecule (*9, 10*) have shown that the critical phenomena can also be observed in an asymmetric top molecule. For molecules with C_{2v} symmetry they can result in fourfold clusterization of rotational energy levels beginning with a certain critical value of the total angular momentum J_{CR} instead of ordinary twofold degeneracy of levels for that type of molecules. The observation of critical phenomena for the water molecule would be rather complicated since the structural rearrangement of the spectrum begins with $J \sim 30$. This follows from both classical estimates (*9*) and quantum model calculations (*10*). The situation is similar for the H_2S molecule (*11*). It was found that H_2Se is a more realistic candidate for an observation of the clusterization effect. It will be shown below that there are two reasons for this. A molecule should be nonrigid and quasisymmetric for the critical phenomena to occur. We estimate that the rearrangement of the rotational spectrum of the H_2Se molecule should begin with $J_{CR} \sim 12$. J_{CR} of H_2Te is even smaller but this molecule is very active and unstable.

High resolution spectra of H_2Se were investigated in a number of papers. MW investigations of the pure rotational spectrum in the ground state were made by Jache,

0022-2852/92 $3.00

Moser, and Gordy (*12*) and Helminger and De Lucia (*13*). Gillis and Edwards (*14*) studied the $2\nu_2$, ν_1, and ν_3 bands, while Lane *et al.* (*15*) analyzed the ν_2 band in the IR region. It should be noted that until the present work there were no data available for the rotational levels in the region of critical phenomena. The previous MW measurements were carried out up to $J = 9$. IR data have rather high J (up to $J = 18$) but small K_{-1} while the spectral rearrangement in H_2Se takes place at the top of J-multiplets, i.e., $K_{-1} \sim J$.

In the present communication the pure rotational spectrum of H_2Se in the ground vibrational state in the submillimeter-wave region is investigated. Detailed measurements in the region of the critical phenomena were made and fourfold clustering of rotational levels was found and traced up to $J = 20$ for two main selenium isotopes. Combined analysis of our and earlier obtained (*12, 13*) MW measurements was undertaken together with analysis of IR ground state combination differences (GSCD) from (*14, 15*) and sets of spectroscopic parameters for $H_2{}^{80}Se$ and $H_2{}^{78}Se$ were obtained.

CRITICAL PHENOMENON IN THE H_2Se ROTATIONAL SPECTRUM

The rotational cluster structure of a molecular spectrum is easily visualized by means of the rotational energy surface (RES) using a classical analog of the effective rotational Hamiltonian (*3*). The classical interpretation of the cluster structure of the rotational spectrum of a spherical top molecule was done for the first time by Dorney and Watson (*2*). Harter and Patterson have shown numerically that the RES topology defines precisely the cluster structure of the rotational spectrum (*3*). They calculated the energy of the level clusters by a semiclassical quantizing of the trajectories on the RES and the cluster splitting using the tunneling integrals between equivalent classical trajectories.

In brief, the RES is the dependence of the rotational energy for the given J on the polar coordinates in the molecular body frame. An example of RES of an asymmetric top molecule is the H_2Se RES shown in Fig. 1(a). There are three twofold axes corresponding to the principal molecular moments of inertia. The moment of inertia with respect to the a-axis is minimal, so the RES maxima lie on the a-axis (as for H_2O, the a-axis is perpendicular to the axis of molecular symmetry). By analogy, minima of RES lie on the c-axis (the c-axis is perpendicular to the molecular plane). The vector of the total angular momentum J precesses around these two axes along the trajectories on RES (*16*). The regions of precession are separated by the separatrix S_h. Since the rotational Hamiltonian of the isolated vibrational state has inversion symmetry, there are pairs of equivalent precessions around the stationary axis (a-axis or c-axis) with the same energies. The classical equienergetic motions have a quantum analogy in degenerate clusters of levels. In this case the pairs of equienergetic motions correspond to double degenerate levels. The cluster splitting of levels is defined by tunneling from one motion to another (*3*). Figure 2 presents the structure of rotational energy levels of an asymmetric top molecule with J ranging from 5 to 34 (only eight upper levels of each J-multiplet relative to J(J, 0) levels are shown). The rotational energies in Fig. 2 are calculated using only the H_2Se A, B and C constants, i.e., without taking into account centrifugal distortion. One can readily see the process of twofold clustering (the two upper levels are practically indistinguishable from $J = 7$).

For detailed analysis of precession around the a-axis we consider the Hamiltonian

$$H = A^{EF} * J^2 + (B - A)^{EF} * J_b^2 + (C - A)^{EF} * J_c^2, \qquad (1)$$

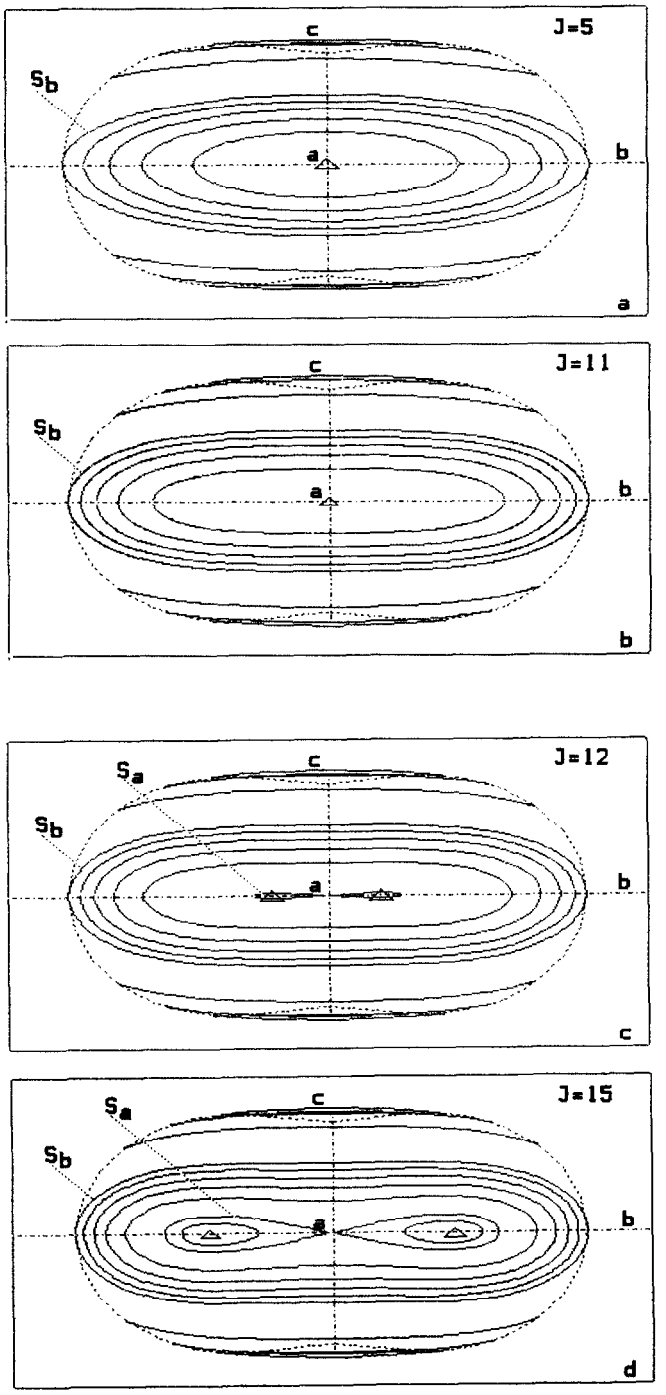

FIG. 1. Trajectories of the total angular momentum vector J on RES for different J: (a) $J = 5$, (b) $J = 11$, (c) $J = 12$, (d) $J = 15$. The a-, b-, and c-axes correspond to the H_2Se principal moments of inertia. S_a and S_b are separatrices.

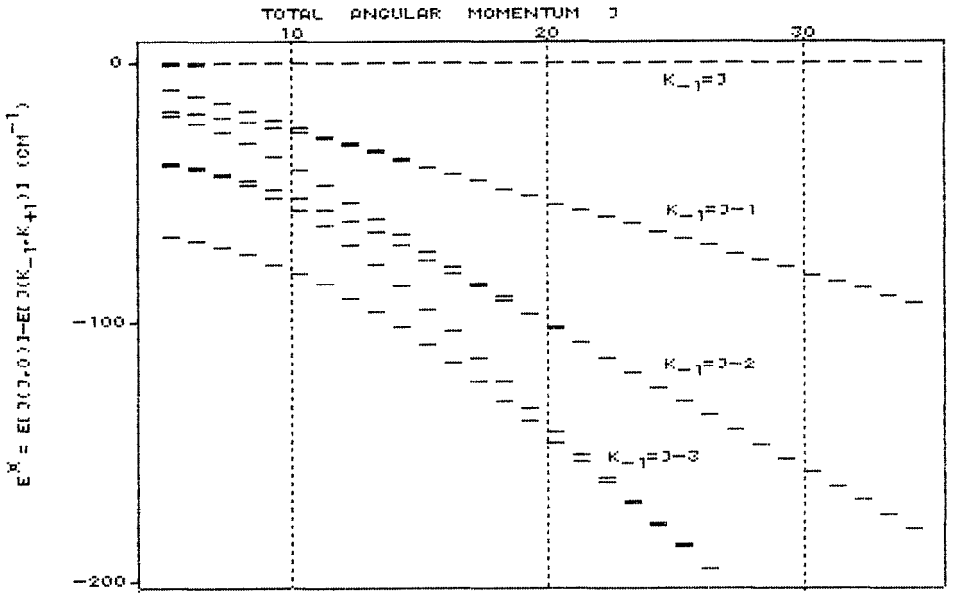

FIG. 2. Rotational level structure of the high K_{-1} part of J-multiplets calculated in a rigid rotor model with H_2Se A, B, C constants. The energy of eight upper levels from $J(J, 0)$ to $J(J-3, 4)$ is presented relative to $J(J, 0)$ levels of each J-multiplet.

where A^{EF}, $(B-A)^{EF}$, and $(C-A)^{EF}$ are functions of J. It is correct in the small neighborhood of the a-axis. For a rigid top Eq. (1) reduces to the strict equation

$$H = A*J^2 + (B-A)*J_b^2 + (C-A)*J_c^2. \tag{2}$$

If $(B-A)^{EF}$ and $(C-A)^{EF}$ are negative the trajectories of precession around the a-axis are ellipses as in Fig. 1(a, b). From the viewpoint of catastrophe theory (*17*) Eq. (1) is valid for all J except for the cases when $(B-A)^{EF}$ or $(C-A)^{EF}$ is zero.

The equilibrium angle of the H_2Se molecule is slightly larger than 90° and its rotational constants A and B are rather close. Due to centrifugal distortion $(B-A)^{EF}$ changes its sign at $J \sim 12$. According to the classification of critical phenomena (*17*) this fact is a local critical phenomenon with C_{2v} symmetry and as a consequence it needs the Hamiltonian

$$H = A^{EF}*J^2 + a*(J-J_{CR})*J_b^2 + b*J_c^2 + t*J_b^4 \tag{3}$$

for the description of the classical motion in the region close to J_{CR} (strictly speaking the coordinate systems of Eqs. (1) and (3) are slightly different). Therefore, even in the immediate neighborhood of the a-axis higher order terms are necessary.

To estimate J_{CR} of H_2Se we can use the rotational and centrifugal distortion constants of a standard A-reduced Hamiltonian in the I^R coordinate representation (*1*), since divergence in it begins with J higher than 30. Reducing a standard Watson Hamiltonian to Eq. (1) we obtain that $(B-A)^{EF}$ is approximately equal to

$$(B-A)^{EF} = (B-A) + (D_{JK} + 2D_K - 2d_J - 2d_K)*J^2. \tag{4}$$

Equation (4) yields the value of $J_{CR} = 11.5$. Since this value corresponds to relatively slight centrifugal distortions in H_2Se we can use the Aliev formulae (*18*) for triatomic

molecules and estimate J_{CR} directly from the rotational constants and vibrational frequencies. Having made some simplifications we obtain

$$J_{CR} = \frac{\omega}{4A}\sqrt{\frac{A-B}{C}}, \tag{5}$$

where ω is the frequency of the bending vibration. This formula is physically clear and gives approximately the same value of $J_{CR} = 10.6$. The first factor characterizes the energy relations of bending vibration and rotation (or nonrigidity), while the second one characterizes the extent of the molecular asymmetry.

One can see from the H_2Se rotational energy surface in Fig. 1(c) that the bifurcation actually appears at $J \sim 12$. It leads to the occurrence of the separatrix S_a and two new stationary axes corresponding to maxima on RES. This catastrophe should result in tunneling splitting between the rotational levels in the localized regions (i.e., the regions inside the separatrix S_a) in the corresponding quantum system. Since there are four equivalent motions in the localized regions, fourfold clusters of the rotational levels will appear. The observation of these essentially qualitative changes in the H_2Se rotational spectrum is the purpose of the present investigation.

EXPERIMENTAL DETAILS AND ASSIGNMENT

We made measurements in the region 300–650 GHz using spectrometers with BWO and an acoustic detector (*19*) (RAD spectrometer). The precision of measurements was 100 kHz for the RAD spectrometer with the submillimeter frequency synthesizer (RAD-2) (*20*) and 300 kHz for the RAD-3 spectrometer (*21*). The line shift was not controlled on every line since observations and estimations show that it is essentially smaller than the accuracy of our data. The pressure in a stainless steel cell was about 0.2–0.6 Torr. In our sample we identified impurity lines of small amounts of H_2O and H_2S. It should be noted that the H_2O and H_2S linewidths are several times broader than those of H_2Se.

There are six selenium isotopes and, thus, six isotopic modifications of H_2Se. A specific line group of the H_2Se rotational spectrum recorded using the RAD-3 spectrometer is presented in Fig. 3. The group character of the spectrum was very useful for line identification. We have measured mostly the Q-type transitions of H_2Se. The most interesting part of them are transitions of the type $J(J, 0) \leftarrow J(J-1, 1)$ and $J(J, 1) \leftarrow J(J-1, 2)$ because the levels involved in these transitions are clustered within the increase of J beginning with $J = 13$. This "cluster" transitions were traced up to $J = 20$. The line intensities of the transitions with $J = 19, 20$ were weak due to a small Boltzmann factor. For example, the line intensity of the transition $20(20, 0) \leftarrow 20(19, 1)$ of the most abundant selenium isotope is about $2. \times 10^{-8}$ cm^{-1}, so to measure these frequencies we heated the cell up to 50–60°C. This temperature was enough to increase the line intensity 3–4 times. The temperature dependence of the line intensity was an additional criterion for line assignment. The H_2Se lines were assigned taking into account frequency and line intensity predictions. The line intensities were estimated in the experiment by comparing them with the well-known neighboring H_2Se lines. The main difficulty in the line intensity estimations is the BWO power dependence on frequency, but nevertheless the error of comparison of neighboring lines does not exceed a factor of 2.

This communication presents only measurements of pure rotational spectra of $H_2{}^{80}Se$ and $H_2{}^{78}Se$ in the ground vibrational state contained in Tables I and II. Analysis

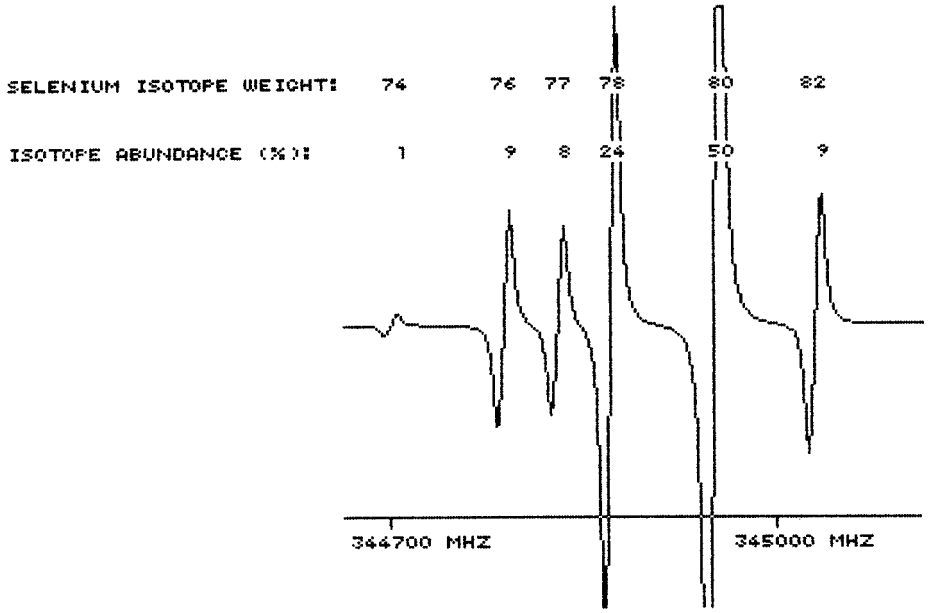

FIG. 3. Part of the H_2Se spectrum recorded using the RAD-3 spectrometer. The isotopic group of 2(1, 1) ← 2(0, 2) transitions of the ground state is presented.

of rotational spectra of the other four isotopes and rotational spectra in the first excited vibrational state will be reported elsewhere.

ANALYSIS OF DATA FITTING

Following Strow (*22*) and Lane *et al.* (*15*) we have used the A-reduced effective rotational Hamiltonian (*1*) in the I^R coordinate representation ($a = z$, $b = x$, $c = y$) in spite of the fact that the H_2Se molecule is nearly an oblate asymmetric top. As in the cases of other H_2X-type molecules we face the problem of slow convergence in a series of the effective rotational Hamiltonian (*23*). The experimental accuracy in fitting all MW frequencies and IR GSCD of H_2Se could be achieved only with 37 parameters in a conventional Watson Hamiltonian

$$\begin{aligned} H = {} & (B + C)/2*J^2 + (A - (B + C)/2)*J_z^2 - D_J*J^4 - D_{JK}*J^2*J_z^2 - D_K*J_z^4 \\ & + H_J*J^6 + H_{JK}*J^4*J_z^2 + H_{KJ}*J^2*J_z^4 + H_K*J_z^6 + L_J*J^8 + L_{JJK}*J^6*J_z^2 \\ & + L_{JK}*J^4*J_z^4 + L_{KKJ}*J^2*J_z^6 + L_K*J_z^8 + P_J*J^{10} + P_{JJK}*J^8*J_z^2 \\ & + P_{JK}*J^6*J_z^4 + P_{KJ}*J^4*J_z^6 + P_{KKJ}*J^2*J_z^8 + P_K*J_z^{10} + Q_{KKJ}*J^2*J_z^8 \\ & + Q_K*J_z^{10} + \tfrac{1}{2}[\{(B - C)/4 - d_J*J^2 - d_K*J_z^2 + h_J*J^4 + h_{JK}*J^2*J_z^2 \\ & + h_K*J_z^4 + l_J*J^6 + l_{JK}*J^4*J_z^2 + l_{KJ}*J^2*J_z^4 + l_K*J_z^6 + p_J*J^8 \\ & + p_{JJK}*J^6*J_z^2 + p_{JK}*J^4*J_z^4 + p_{KKJ}*J^2*J_z^6 + p_K*J_z^8\}, \{J_+^2 + J_-^2\}]_+. \end{aligned} \quad (6)$$

However, analysis of the fitted data showed that there are no data with high J and mean K_{-1} and the number of parameters can be reduced. We transform the standard Hamiltonian into

$$H = H_d + \tfrac{1}{2}[H_{nd}, (J_+^2 + J_-^2)]_+$$

$$H_d = \sum_{m,n} c_{mn} * (J^2 - J_z^2)^m * J_z^{2n}$$

$$H_{nd} = \sum_{m,n} b_{mn} * (J^2 - J_z^2)^m * J_z^{2n}, \qquad (7)$$

where similarly to Eq. (6) $[A, B]_+ = AB + BA$. There are the following relationships between the parameters of Eqs. (6) and (7): $c_{10} = (B + C)/2$, $c_{01} = A$, $b_{00} = (B - C)/4$, $c_{20} = -D_J$, $c_{11} = -2D_J - D_{JK}$, $c_{02} = -D_J - D_{JK} - D_K$, etc. This reduction does not differ from that of Watson. Using simple arithmetic operations one can easily transform Eq. (7) into Eq. (6) and back, so there is strict correspondence between the parameters of these two kinds of Hamiltonians. The use of model (7) in fit leads to uncertainties of some constants exceeding the constants themselves (Table III). So we set seven parameters to zero and achieved a standard deviation equal to unity with only 30 parameters in the Hamiltonian. It is remarkable that the centrifugal distortion constants in our Hamiltonian are 10 or even 100 times smaller than in model (6) (see Table III). The advantage of model (7) is that only the c_{0n} and b_{0n} constants are necessary in case $K_{-1} \sim J$, contrary to model (6) where all the constants are essential.

Hamiltonian (7) was introduced especially for better determination and reduction of the parameters. So in the final fitting we used the Hamiltonian

$$\begin{aligned} H = {} & (B + C)/2 * J^2 + (A - (B + C)/2) * J_z^2 - D_J * J^4 - D_{JK} * J^2 * J_z^2 - D_K * J_z^4 \\ & + H_J * J^6 + H_{JK} * J^4 * J_z^2 + H_{KJ} * J^2 * J_z^4 + H_K * J_z^6 + c_{40} * (J^2 - J_z^2)^4 \\ & + c_{31} * (J^2 - J_z^2)^3 * J_z^2 + c_{22} * (J^2 - J_z^2)^2 * J_z^4 + c_{13} * (J^2 - J_z^2) * J_z^6 + c_{04} * J_z^8 \\ & + c_{50} * (J^2 - J_z^2)^5 + c_{32} * (J^2 - J_z^2)^3 * J_z^4 + c_{05} * J_z^{10} + \tfrac{1}{2}[\{(B - C)/4 \\ & - d_J * J^2 - d_K * J_z^2 + h_J * J^4 + h_{JK} * J^2 * J_z^2 + h_K * J_z^4 + b_{30} * (J^2 - J_z^2)^3 \\ & + b_{21} * (J^2 - J_z^2)^2 * J_z^2 + b_{03} * J_z^6 + b_{40} * (J^2 - J_z^2)^4 + b_{13} (J^2 - J_z^2) * J_z^6 \\ & + b_{04} * J_z^8\}, \{J_+^2 + J_-^2\}]_+, \end{aligned} \qquad (8)$$

where the parameters with terms of total power six and lower are the same as in the ordinary Watson A-reduction, whereas higher terms are reformulated according to Eq. (7).

Tables I and II present lists of $H_2{}^{80}Se$ and $H_2{}^{78}Se$ MW frequencies fitted in model (8), respectively. The rotational and centrifugal distortion constants given in Table IV reproduce MW data and IR GSCD with experimental accuracy. We should note that MW frequencies of Refs. (*12, 13*) have been fitted here with uncertainties smaller by a factor of two. IR GSCD uncertainties were taken as $\sigma_i = 90.\ \mathrm{MHz}/\sqrt{P_i}$, where P_i are IR GSCD weights (*15*). The standard deviation was defined as

$$\text{Std. Dev.} = \sqrt{\sum_i^N \frac{(V_i^{\text{obs}} - V_i^{\text{calc}})^2}{\sigma_i^2}} \Big/ N.$$

Some characteristics of fitted data are summarized in Table V.

DISCUSSION

As mentioned above the main goal of this work is the observation of the rotational level clusterization in H_2Se with increasing J. The critical phenomenon should change

TABLE I

Observed $H_2{}^{80}Se$ MW Lines Fitted in Model (8)

FREQ.	O.-C.	UNC.	J'	KA'	KC'	J"	KA"	KC"
127973.40 a	-0.14	0.10	1	1	0	1	0	1
142171.86 a	-0.19	0.10	2	2	0	2	1	1
165240.46 a	0.10	0.10	3	3	0	3	2	1
198776.38 b	0.07	0.10	4	4	0	4	3	1
243754.69 b	0.00	0.10	5	5	0	5	4	1
299490.16 b	-0.02	0.10	6	6	0	6	5	1
302316.34	-0.06	0.10	20	20	1	20	19	2
305959.97	-0.03	0.10	6	1	5	5	4	2
307884.72 b	0.04	0.10	5	4	1	5	3	2
309399.66 b	0.03	0.10	6	5	1	6	4	2
316164.20 b	0.03	0.10	4	3	1	4	2	2
324255.52 b	-0.01	0.10	7	6	1	7	5	2
329992.71 b	-0.04	0.10	3	2	1	3	1	2
336187.70	-0.24	0.50	3	1	3	2	2	0
344953.15 b	0.02	0.10	2	1	1	2	0	2
350168.40	-0.66	0.70	6	2	5	5	3	2
355087.30 b	-0.08	0.10	8	7	1	8	6	2
361879.28 b	0.02	0.10	1	1	1	0	0	0
362998.90 b	-0.10	0.10	7	7	0	7	6	1
373816.77	0.24	0.10	19	19	0	19	18	1
375107.10	0.37	1.00	19	19	1	19	18	2
383463.65 b	0.06	0.10	2	2	1	2	1	2
402553.93 b	0.04	0.10	3	3	1	3	2	2
403259.55 b	-0.14	0.10	9	8	1	9	7	2
427295.16 b	-0.02	0.10	4	4	1	4	3	2
429235.84 b	-0.07	0.10	8	8	0	8	7	1
443219.07	-0.21	0.10	18	18	0	18	17	1
445382.77	-0.07	0.10	18	18	1	18	17	2
456827.96 b	-0.07	0.10	5	5	1	5	4	2
468076.44	-0.01	0.10	10	9	1	10	8	2
474150.38	-0.06	0.10	10	8	2	10	7	3
479412.00	0.04	0.10	9	7	2	9	6	3
487728.67	-0.02	0.10	11	9	2	11	8	3
489861.69 b	-0.08	0.10	6	6	1	6	5	2
492152.55 b	0.01	0.10	9	9	0	9	8	1
498190.96	-0.01	0.10	8	6	2	8	5	3
505083.14	-0.06	0.10	17	17	0	17	16	1
508610.32	0.01	0.10	17	17	1	17	16	2
523529.04	0.06	0.10	12	10	2	12	9	3
524110.61	-0.03	0.10	7	5	2	7	4	3
524657.70	-0.01	0.10	7	7	1	7	6	2
546105.71	0.12	0.10	11	10	1	11	9	2
546126.71	-0.05	0.10	10	10	0	10	9	1
550936.68	-0.11	0.10	6	4	2	6	3	3
555879.55	0.32	0.20	16	16	0	16	15	1
559092.56	0.08	0.10	8	8	1	8	7	2
561525.26	0.12	0.10	16	16	1	16	15	2
573860.60	-0.13	0.10	5	3	2	5	2	3
581098.89 b	0.01	0.10	2	0	2	1	1	1
582078.18	-0.02	0.10	13	11	2	13	10	3
587082.69	0.02	0.10	11	11	0	11	10	1
590368.96	-0.10	0.10	4	2	2	4	1	3
590794.17	0.14	0.10	9	9	1	9	8	2
593231.88	0.06	0.10	15	15	0	15	14	1
595800.97 b	0.01	0.10	2	1	2	1	0	1
600323.16	-0.05	0.10	3	1	2	3	0	3
602159.26	0.12	0.10	15	15	1	15	14	2
606976.36	0.08	0.10	3	2	2	3	1	3

TABLE I—*Continued*

FREQ.	O.-C.	UNC.	J' KA' KC'	J" KA" KC"
609360.34	0.09	0.10	4 3 2	4 2 3
612767.52	0.13	0.10	12 12 0	12 11 1
614973.03	0.04	0.10	5 4 2	5 3 3
615663.22	-0.05	0.10	14 14 0	14 13 1
617320.05	0.10	0.10	10 10 1	10 9 2
622313.85	-0.17	0.10	13 13 0	13 12 1
624973.38	0.09	0.10	6 5 2	6 4 3
629639.40	-0.08	0.10	14 14 1	14 13 2
631533.60	-0.04	0.10	12 11 1	12 10 2
635018.71	0.00	0.10	14 11 3	14 10 4
635737.46	-0.01	0.10	13 10 3	13 9 4
636338.42	-0.01	0.10	11 11 1	11 10 2
640271.35	0.13	0.10	7 6 2	7 5 3
643956.43	-0.14	0.10	13 13 1	13 12 2
645781.02	0.04	0.20	12 12 1	12 11 2

[a] Ref. (12)
[b] Ref. (31)

the rotational levels structure in Fig. 2 and result in the fourfold clustering of levels. So the frequency increase of the subbranches $J(J, 0) \leftarrow J(J-1, 1)$ and $J(J, 1) \leftarrow J(J-1, 2)$ of the Q branch should be changed to a frequency decrease after the critical phenomenon occurs. When our measurements were performed up to 650 GHz it was found out indeed that the frequencies of those "cluster" subbranches increase with J up to $J = 12$ and begin to decrease from $J = 13$. This fact is one of the main results of our work and means that the clusterization in H_2Se really takes place. The $H_2{}^{80}Se$ rotational levels are presented in Fig. 4. Some observed transitions are shown by dotted lines. As in Fig. 2 only eight upper rotational levels of J-multiplets with $J = 5$–34 are given. The difference between Fig. 2 and Fig. 4 is evident: the fourfold clusters of the rotational levels are easily observed in Fig. 4.

The problem of the dependence of the rate of the clusterization procedure on J is very important and interesting as well. It was pointed out in Ref. (*17*) that the cluster splitting should decrease exponentially with increasing J. By measuring $J(J, 0) \leftarrow J(J-1, 1)$ and $J(J, 1) \leftarrow J(J-1, 2)$ transition frequencies (see Fig. 4) we defined the size of the upper fourfold cluster for different values of J with very high accuracy. Fig. 4 shows that first the cluster size decreases linearly and then beginning with $J = 18$ exponentially when all four upper levels are in local regions. For $J = 20$ the measured size of the cluster is five times smaller than the distance to the nearest level of the same J-multiplet.

We have mentioned above that the H_2Se rotational Hamiltonian converges slowly and diverges beginning with J larger than 33. It has been shown (*23*) that one-dimensional approximation of effective rotational Hamiltonians is a very useful tool in the case of divergent Hamiltonians. We have found that this approach is also relevant when high J levels of H_2Se are treated. For example, we applied one-dimensional approximation in the Padé form to the conventional model with terms up to the eighth power and decreased the standard deviation six times. However, the clusterization of rotational levels is a very fine effect and we reproduce the predictions in Fig. 4 only

TABLE II

Observed $H_2{}^{78}Se$ MW Lines Fitted in Model (8)

FREQ.		O.-C.	UNC.	J'	KA'	KC'	J"	KA"	KC"
142469.58	a	0.04	0.10	2	2	0	2	1	1
165847.57	a	-0.28	0.10	3	3	0	3	2	1
199858.66	b	0.13	0.10	4	4	0	4	3	1
245484.52	b	0.04	0.10	5	5	0	5	4	1
301999.28	b	-0.03	0.10	6	6	0	6	5	1
305852.35		0.01	0.10	6	1	5	5	4	2
307754.78	b	0.05	0.10	5	4	1	5	3	2
308377.25		-1.21	0.50	20	20	1	20	19	2
309568.45	b	0.09	0.10	6	5	1	6	4	2
315928.10	b	-0.07	0.10	4	3	1	4	2	2
324938.27	b	0.06	0.10	7	6	1	7	5	2
329795.90	b	-0.06	0.10	3	2	1	3	1	2
336236.30		-0.33	0.50	3	1	3	2	2	0
344872.29	b	-0.05	0.10	2	1	1	2	0	2
356498.41	b	-0.03	0.10	8	7	1	8	6	2
362069.14	b	-0.02	0.10	1	1	1	0	0	0
366331.05	b	-0.16	0.10	7	7	0	7	6	1
380453.55		0.12	0.10	19	19	0	19	18	1
381699.48		0.58	0.30	19	19	1	19	18	2
383819.46	b	0.08	0.10	2	2	1	2	1	2
403153.22	b	0.06	0.10	3	3	1	3	2	2
405571.85	b	-0.10	0.10	9	8	1	9	7	2
428221.28	b	0.06	0.10	4	4	1	4	3	2
450141.07		-0.30	0.20	18	18	0	18	17	1
452229.19		-0.10	0.10	18	18	1	18	17	2
458160.01	b	-0.04	0.10	5	5	1	5	4	2
471356.11		-0.02	0.10	10	9	1	10	8	2
474165.36		-0.10	0.10	10	8	2	10	7	3
478837.38		-0.01	0.10	9	7	2	9	6	3
488674.13		0.03	0.10	11	9	2	11	8	3
491668.90		-0.07	0.10	6	6	1	6	5	2
496878.95		-0.01	0.10	9	9	0	9	8	1
497368.19		0.03	0.10	8	6	2	8	5	3
512069.04		-0.14	0.10	17	17	0	17	16	1
515475.03		-0.03	0.20	17	17	1	17	16	2
523325.24		0.01	0.10	7	5	2	7	4	3
525690.12		0.06	0.10	12	10	2	12	9	3
526993.44		-0.01	0.10	7	7	1	7	6	2
550256.45		0.06	0.10	11	10	1	11	9	2
550370.01		-0.08	0.10	6	4	2	6	3	3
551334.19		0.07	0.10	10	10	0	10	9	1
561990.45		0.02	0.10	8	8	1	8	7	2
562770.37		0.21	0.10	16	16	0	16	15	1
568229.49		0.10	0.20	16	16	1	16	15	2
573572.04		-0.11	0.10	5	3	2	5	2	3
581180.62	b	0.09	0.10	2	0	2	1	1	1
585613.69		-0.03	0.10	13	11	2	13	10	3
590319.07		-0.09	0.10	4	2	2	4	1	3
592658.56		0.08	0.10	11	11	0	11	10	1
594267.54		0.12	0.10	9	9	1	9	8	2
596061.86	b	-0.07	0.10	2	1	2	1	0	1
599927.31		-0.05	0.10	15	15	0	15	14	1
600425.47		-0.03	0.10	3	1	2	3	0	3
607199.21		0.08	0.10	3	2	2	3	1	3
608576.25		0.14	0.10	15	15	1	15	14	2
609644.84		0.07	0.10	4	3	2	4	2	3
615372.85		0.05	0.10	5	4	2	5	3	3
618652.15		-0.04	0.10	12	12	0	12	11	1

TABLE II—*Continued*

FREQ.	O.-C.	UNC.	J'	KA'	KC'	J"	KA"	KC"
621363.97	0.06	0.10	10	10	1	10	9	2
622108.83	0.01	0.10	14	14	0	14	13	1
625555.29	0.06	0.10	6	5	2	6	4	3
628485.13	-0.10	0.10	13	13	0	13	12	1
634946.36	0.01	0.10	13	10	3	13	9	4
635350.30	-0.01	0.10	14	11	3	14	10	4
635681.01	-0.05	0.10	14	14	1	14	13	2
636298.57	-0.02	0.10	12	11	1	12	10	2
640934.06	0.02	0.10	11	11	1	11	10	2
641108.43	0.04	0.10	7	6	2	7	5	3
649560.05	-0.03	0.10	13	13	1	13	12	2
650899.08	-0.12	0.10	12	12	1	12	11	2

[a] Ref. (12)
[b] Ref. (31)

TABLE III

Comparison of the $H_2{}^{80}Se$ Fitting Parameters of High Power Terms Obtained by the Conventional Model (6), and the Modified Watson Hamiltonian (7)

MODEL (6)		MODEL (7)	
$P_J *10^8$	-3.6(0.1)[a]	0.6(0.1)	$c_{50}*10^8$
$P_{JJK}*10^8$	7.6(0.5)	1.0(0.3)	$c_{41}*10^8$
$P_{JK} *10^8$	18.(3.)	8.(2.)	$c_{32}*10^8$
$P_{KJ} *10^8$	-138.(7.)	-2.(5.)	$c_{23}*10^8$
$P_{KKJ}*10^8$	165.(9.)	0.8(1.)	$c_{14}*10^8$
$P_K *10^8$	-55.(4.)	1.9(0.3)	$c_{05}*10^8$
$P_J *10^8$	-1.90(0.06)	0.26(0.07)	$b_{40}*10^8$
$P_{JJK}*10^8$	-5.8(0.3)	-0.4(0.6)	$b_{31}*10^8$
$P_{JK} *10^8$	-11.(1.)	-0.6(2.)	$b_{22}*10^8$
$P_{KKJ}*10^8$	48.(3.)	4.(1.)	$b_{13}*10^8$
$P_K *10^8$	-20.(2.)	2.00(0.06)	$b_{04}*10^8$
$Q_{KKJ}*10^{11}$	-40.5(0.9)	3.(1.)	$c_{15}*10^{11}$
$Q_K *10^{11}$	38.1(0.8)	-0.67(0.03)	$c_{06}*10^{11}$
Number of parameters	37	37	
MW Std. Dev.	1.92	0.65	
IR GSCD Std. Dev.	1.10	0.95	
TOTAL Std. Dev.	1.24	0.92	

[a] Value in parentheses is one standard deviation.

TABLE IV

Rotational and Centrifugal Distortion Constants of $H_2{}^{80}Se$ and $H_2{}^{78}Se$ obtained in Model (8)

	$H_2{}^{80}Se$	$H_2{}^{78}Se$
(B+C)/2	174306.123(22)[a]	174324.017(28)
A-(B+C)/2	70620.170(18)	70756.666(20)
(B-C)/2	57339.680(15)	57322.047(16)
D_J	15.8381(10)	15.8417(29)
D_{JK}	-55.4309(39)	-55.4429(47)
D_K	79.0432(24)	79.1035(30)
d_J	7.27025(82)	7.27044(95)
d_K	-5.4957(14)	-5.4809(16)
$H_J *10^3$	6.519(26)	6.613(63)
$H_{JK}*10^3$	-37.19(13)	-37.73(24)
$H_{KJ}*10^3$	38.35(23)	39.12(36)
$H_K *10^3$	13.48(13)	13.18(18)
$h_J *10^3$	3.234(17)	3.196(28)
$h_{JK}*10^3$	-12.200(51)	-11.995(93)
$h_K *10^3$	23.571(63)	23.425(90)
$c_{40}*10^6$	-4.62(17)	-5.16(36)
$c_{31}*10^6$	14.97(35)	16.5(15)
$c_{22}*10^6$	-14.3(14)	-13.0(24)
$c_{13}*10^6$	19.6(11)	20.0(17)
$c_{04}*10^6$	-17.82(21)	-17.66(36)
$b_{30}*10^6$	-2.105(92)	-1.82(18)
$b_{21}*10^6$	4.83(37)	4.18(60)
$b_{03}*10^6$	-24.13(23)	-24.16(30)
$c_{50}*10^9$	3.85(26)	4.91(61)
$c_{32}*10^9$	19.5(34)	19.5[b]
$c_{05}*10^9$	16.88(17)	16.58(16)
$b_{40}*10^9$	1.45(12)	0.94(30)
$b_{13}*10^9$	20.51(95)	17.6(21)
$b_{04}*10^9$	21.90(37)	21.96(50)
$c_{06}*10^{12}$	-7.78(12)	-7.63(12)
MW Std.Dev.	0.99	0.90
Std.Dev. of IR GSCD	0.96	1.12
Total Std.Dev.	0.96	1.09

[a] Value in parentheses is one standard deviation in last digits of parameter.
[b] Value was fixed to the corresponding value for $H_2{}^{80}Se$.

TABLE V

Some Characteristics of Fitted Data

Selenium Isotope	80	78
Number of IR Ground State Combination Differencies	510	355
Number of Earlier Measured MW Lines	25	21
Total Number of MW Lines	73	70
J max	20	20
Ka max	20	20
Kc max	18	17
MW Std. Dev.	0.99	0.90
IR GSCD Std. Dev.	0.96	1.12
Total Std. Dev.	0.96	1.09

up to the point of divergence up to which the predictions in different models are qualitatively similar. According to Fig. 4 the cluster splitting decreases exponentially and the formation of the second cluster starts with further increase of J; i.e., the process of fourfold clusterization involves more and more levels.

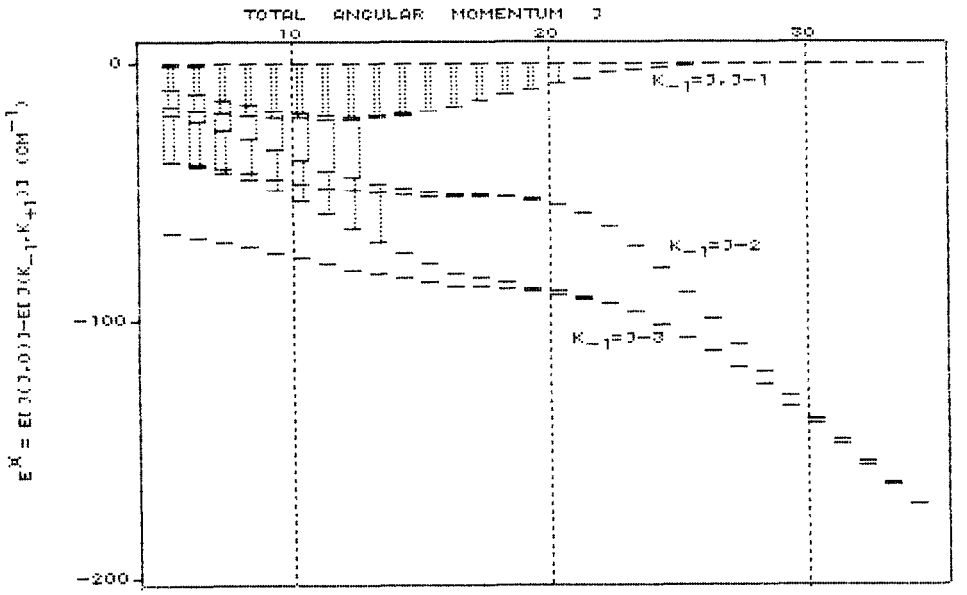

FIG. 4. The H_2Se rotational level structure of the high K_{-1} part of J-multiplets. The energy of eight upper levels from $J(J, 0)$ to $J(J-3, 4)$ is presented relative to $J(J, 0)$ levels of each J-multiplet. Some experimentally observed Q-type transitions are shown by dotted lines.

The newborn stationary axes move with J growth towards the b-axes (Fig. 1c, d). Having analyzed rotational energy surfaces based on a Hamiltonian with experimentally derived constants, we realized that at high J the axes' locations are stabilized. The dependence of the angle between the new stationary and a-axes on J is shown in Fig. 5. This dependence is in good agreement with the simple formula for an A_2B molecule taken from Ref. (*24*) (dotted line)

$$\phi = \arcsin \sqrt{\frac{1 - J_{CR}^2/J^2}{2(1 + m/M)}} \tag{9}$$

where m is the mass of the A atom and M is the mass of the B atom. It is evident from the experimental dependence (solid line) that the stabilization angle is about 40°. So we can roughly describe the classical picture of molecular dynamics under rotational excitation. When J is lower than 12 the molecule rotates precessing around the a-axis. As a result of centrifugal distortion the axis of precession splits into two axes. This means that the molecule tends to precess around the axis lying along its H-bond, another H-bond being perpendicular to this axis for rather high J. Hence the distortion of the H-bond begins to play an essential role.

One more effect has been observed: very strong distortion of the "cluster" linestrengths in comparison with the rigid rotor approximation. Two kinds of linestrength calculations of the Q-type transitions are presented in Table VI: part A is based on model (8) and the constants of Table IV and part B on the rigid rotor model. Table VI especially shows the differences between the calculations in the above models at

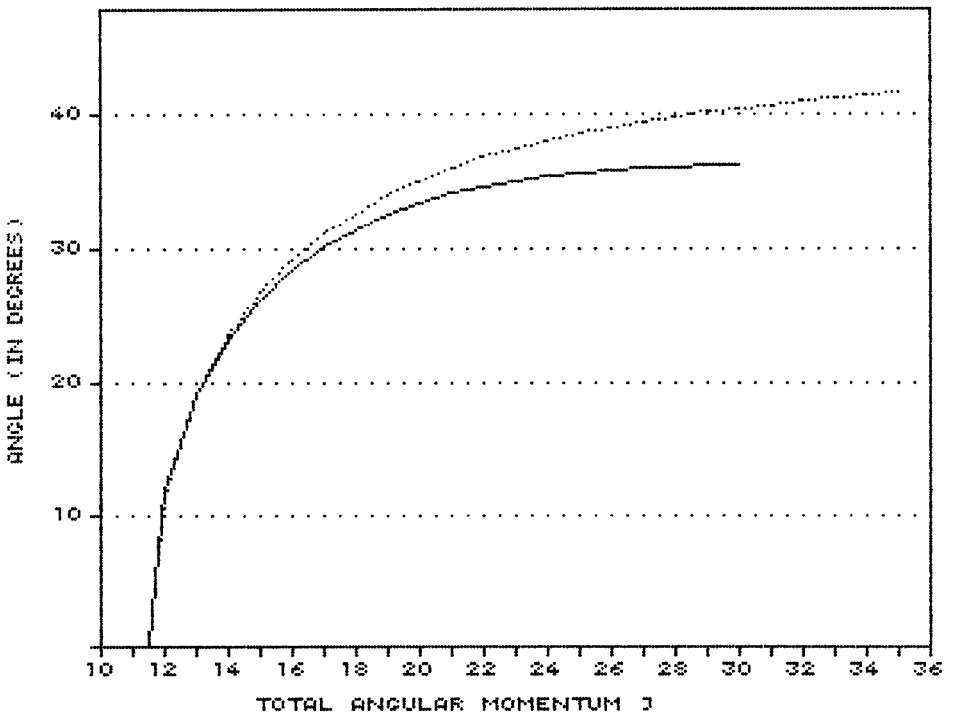

FIG. 5. Experimental dependence of angle between the newborn stationary axis and the a-axis on J (solid line) and the same dependence calculated according to Eq. (9) with $J_{CR} = 11.5$ (dotted line).

TABLE VI

Calculated Linestrengths of Rotational Transitions of H_2Se in Nonrigid (part A) and Rigid Rotor (part B) Models

J	5	10	15	20	25	30
		part A				
J(J ,0) - J(J-1,1)	3.59	3.59	4.83	9.07	16.89	24.62
J(J ,1) - J(J-1,2)	2.21	3.32	4.77	9.05	16.88	24.62
J(J-1,1) - J(J-2,2)	3.94	6.42	5.73	4.32	1.63	0.80
J(J-1,2) - J(J-2,3)	2.37	4.76	5.49	4.30	1.63	0.80
		part B				
J(J ,0) - J(J-1,1)	3.57	3.11	3.07	3.08	3.08	3.09
J(J ,1) - J(J-1,2)	2.20	2.96	3.06	3.08	3.08	3.09
J(J-1,1) - J(J-2,2)	4.00	7.16	6.23	6.14	6.15	6.16
J(J-1,2) - J(J-2,3)	2.39	5.02	5.98	6.13	6.15	6.16

high J. Immediately after the critical phenomenon the linestrengths of the "cluster" transitions begin to increase with J while the "intercluster" line strengths begin to decrease. This coincides with the results of our experiment: estimates of the "cluster" line intensities with respect to the well-known neighboring lines are in good agreement with the part A calculations.

Thus a number of effects under rotational excitation are caused by the critical phenomena in H_2Se. However, the behavior of the fourfold clusters with J larger than 30 is not precisely clear. It is impossible to predict the rotational energy with such high J using conventional Hamiltonians because it becomes divergent due to strong rotational–vibrational interaction. High energy predictions by means of the model Hamiltonians (*10, 11*) take into account the bending vibration only, but the nonrigidity of valence bonds is very important with J larger than J_{CR}, as mentioned above. So the further measurements of the H_2Se "cluster" lines for higher J are extremely interesting and important for understanding of the cluster phenomena. They are important not only for the particular case of H_2Se, but also for the H_2O and H_2S molecules where the clusterization of levels can occur only in the region of the Hamiltonian divergence.

This paper is a detailed representation of the report presented at the International Conference on IR Spectroscopy in Prague (*25*).

ACKNOWLEDGMENTS

The authors are grateful to Drs. B. I. Zhilinskii and I. M. Pavlichenkov for useful discussions. We are thankful to Professor T. H. Edwards for providing us with IR H_2Se data, to Dr. J. T. Hougen for his interest in this work and his help in making the existing data on H_2Se available for us, and to Dr. A. F. Krupnov for helpful comments on the manuscript. We thank Dr. J. Makarewicz for helpful discussions and for sending us his papers before publication.

RECEIVED July 30, 1991

REFERENCES

1. J. K. G. WATSON, *in* "Vibrational Spectra and Structure" (J. Durig, Ed.), Vol. 6, p. 1, Elsevier, Amsterdam, 1977.
2. A. J. DORNEY AND J. K. G. WATSON, *J. Mol. Spectrosc.* **42,** 135–148 (1972).
3. W. G. HARTER AND C. W. PATTERSON, *J. Chem. Phys.* **80,** 4241–4261 (1984).
4. W. G. HARTER AND C. W. PATTERSON, *J. Math. Phys.* **20,** 1453–1459 (1979).
5. I. M. PAVLICHENKOV AND B. I. ZHILINSKII, *Chem. Phys.* **100,** 339–354 (1985).
6. D. A. SADOVSKII, B. I. ZHILINSKII, J. P. CHAMPION, AND G. PIERRE, *J. Chem. Phys.* **92,** 1523–1537 (1990).
7. V. M. KRIVTSUN, D. A. SADOVSKII, AND B. I. ZHILINSKII, *J. Mol. Spectrosc.* **139,** 126–146 (1990).
8. O. I. DAVARACHVILLI, B. I. ZHILINSKII, V. M. KRIVTSUN, D. A. SADOVSKII, AND E. P. SNEGIREV, *Pis'ma Zh. Eksp. Teor. Fiz.* **51,** 17–19 (1990). [In Russian]
9. B. I. ZHILINSKII AND I. M. PAVLICHENKOV, *Opt. Spektrosk.* **64,** 688–690 (1988). [In Russian]
10. J. MAKAREWICZ AND J. PYKA, *Mol. Phys.* **68,** 107–127 (1989); J. MAKAREWICZ, *Mol. Phys.* **69,** 903–921 (1990).
11. J. PYKA, *Mol. Phys.* **70,** 547–561 (1990).
12. A. W. JACHE, P. W. MOSER, AND W. GORDY, *J. Chem. Phys.* **25,** 209 (1956).
13. P. HELMINGER AND F. C. DE LUCIA, *J. Mol. Spectrosc.* **58,** 375–383 (1975).
14. J. R. GILLIS AND T. H. EDWARDS, *J. Mol. Spectrosc.* **85,** 74–84 (1981).
15. WM. C. LANE, T. H. EDWARDS, J. R. GILLIS, F. S. BONOMO, AND F. J. MURCRAY, *J. Mol. Spectrosc.* **107,** 306–317 (1984).
16. L. D. LANDAU AND E. M. LIFSHITZ, "Quantum Mechanics," Pergamon, Oxford, 1965.
17. B. I. ZHILINSKII AND I. M. PAVLICHENKOV, *Zh. Eksp. Teor. Fiz.* **92,** 387–403 (1987) [in Russian]; *Sov. Phys. JETP Engl. Transl.* **65,** 221–229 (1987); I. M. PAVLICHENKOV AND B. I. ZHILINSKII, *Ann. Phys. (N.Y.)* **184,** 1–32 (1988).
18. M. R. ALIEV, *Opt. Spektrosk.* **65,** 986–988, (1988).
19. S. P. BELOV, A. V. BURENIN, L. I. GERSHTEIN, V. V. KOROLIKHIN, AND A. F. KRUPNOV, *Opt. Spektrosk.* **35,** 295–302 (1973). [In Russian]
20. A. F. KRUPNOV, *Vest. Akad. Nauk USSR* **7,** 18–29 (1978).
21. S. P. BELOV, V. M. DEMKIN, V. I. PUTCHENKIN, AND M. YU. TRETYAKOV, "The Third Generation Submillimeterwave Spectrometer RAD," unpublished.
22. L. L. STROW, *J. Mol. Spectrosc.* **97,** 9–28 (1983).
23. O. L. POLYANSKY, *J. Mol. Spectrosc.* **112,** 79–87 (1985).
24. I. M. PAVLICHENKOV, *in* "Phizika Atomnogo Yadra," p. 67, Leningrad, 1989.
25. S. P. BELOV, I. N. KOZIN, O. L. POLYANSKY, AND M. YU. TRETYAKOV, *in* "Proceedings XIth International Conference IR Spectroscopy, Prague, 1990," p. 125.